ETH zürich

ETH Library

A methodology to calculate long-term shallow geothermal energy potential for an urban neighbourhood

Journal Article

Author(s):
Miglani, Somil; Orehounig, Kristina; Carmeliet, Jan

Publication date:
2018-01-15

Permanent link:
https://doi.org/10.3929/ethz-b-000217121

Rights / license:
In Copyright - Non-Commercial Use Permitted

Originally published in:
Energy and Buildings 159, https://doi.org/10.1016/j.enbuild.2017.10.100

This page was generated automatically upon download from the ETH Zurich Research Collection.
For more information, please consult the Terms of use.

A methodology to calculate long-term shallow geothermal energy potential for an urban neighbourhood

Somil Miglani [a,b,*], Kristina Orehounig [a,b], Jan Carmeliet [a]

[a] Chair of building Physics, Swiss Federal Institute of Technology, ETH Zurich, Switzerland

[b] Urban Energy Systems Laboratory, Swiss Federal Laboratories for Materials Science and Technology, EMPA, Duebendorf, Switzerland

*Corresponding author address: Stefano Franscini Platz 1, ETH Hoengerberg, CH 8093. Tel: +41 789 29 03 40

Abstract

Ground source heat pumps typically use Borehole Heat Exchangers (BHEs) which are drilled vertically into the ground to extract heat. Space limitations in urban areas can limit the total length of BHEs. Continuous heat extraction over long period from BHEs especially with limited length results in cooling of the ground. Furthermore, the presence of neighbouring BHEs adds to the cooling effect thereby reducing the overall geothermal energy potential. Therefore, it is important to consider spatial constraints and the thermal interference from neighbouring BHEs when evaluating the geothermal energy potential of urban areas. In this paper, a methodology to calculate the long-term geothermal energy potential for an urban neighbourhood is developed. A GIS based workflow is used to design the BHEs for multiple buildings, in order to satisfy their total heating/cooling demand considering spatial constraints. A model that accounts for thermal interference between neighbouring BHEs is developed to simulate their operation and the long-term geothermal energy potential is calculated. The method is applied to an urban neighbourhood in Zurich, Switzerland with 170 buildings. Results show that the geothermal energy potential is overestimated if thermal interference between BHEs are not accounted for. A long-term declining trend is observed in the geothermal energy potential due to ground cooling.

Keywords: Building energy demand, Borehole heat exchanger, Shallow geothermal energy, GIS, Renewable energy

1. Introduction

1.1 Background

Human induced climate change, depleting fossil fuel reserves and the increasing pressure from the global populace for cleaner sources of energy, are pushing the energy sector towards a transition. The seeds of this transition have been sowed through the development of energy strategies by the world's major economies. For instance, the European Union (EU) is committed to reducing its collective GHG emissions by 20% from the 1990 levels by 2020 [1] and 80-95% by 2050 [2]. These targets are ambitious and necessitate an energy system with an exceptionally high share of renewable energy. Furthermore, contributions are needed from various energy consuming sectors such as buildings, transport, industry, agriculture etc. The building sector in the EU represents 40% of the total final energy use [3] and contributes 36% of CO_2 emissions [4] providing an opportunity to reduce a substantial amount of emissions. The Energy Performance of Buildings Directive, which is the main legislation in the EU for energy efficient buildings also advocates the use of heat pumps and renewable energy for heating and cooling in buildings [5]. Furthermore, the

International Energy Agency (IEA) also recommends the installation of heat pumps for space heating, cooling and domestic hot water (DHW) as an immediate priority [3].

Ground Source Heat Pumps (GSHPs) are a mature technology that has been widely used in buildings for space heating/cooling and DHW production. Recent advances have led to the increase in the energy efficiency of these systems making them an attractive alternative for heating in buildings [6]. In terms of CO_2 emissions and energy efficiency, GSHPs rank higher than all fossil fuel based boilers and their air source counterparts [7]. A GSHP uses the ground, ground water or surface water as its source or sink. There are two main types of GSHP systems, the *closed loop system* and the *open loop system*. In a closed loop system the GSHP is connected to a U-pipe heat exchanger installed underground through which a water or water-antifreeze mixture is circulated to exchange heat with the ground. Borehole Heat Exchangers (BHE) which are drilled vertically into the ground are a commonly used example of such a system. An open loop system draws water directly from the water table or a lake, pond etc. and passes it through the heat pump. There are several other types and configurations of heat exchangers that are used in conjunction with the heat pump, which differ in their design, costs, spatial constraints, installation requirements etc. A detailed description of the different heat exchangers used with GSHPs is described by Florides and Kalogirou [8].

BHEs are ideal for urban areas where surface area is limited and the desire for interference with the landscape is minimal. BHEs can be drilled in the space between the building walls and the parcel boundary. The primary design parameter for each BHE is its total length that determines the possible heat extraction from the ground. The longer the BHE length the higher the possible heat extraction. Contrastingly, the drilling costs increase with every meter drilled. Therefore, a good design of the BHE system should size for the minimum length that is required for satisfying the total thermal energy demand. For high heating and cooling demands, there may be a need for installation of multiple BHEs to achieve long lengths connected to a single heat pump supplying heat to a building. In that case, the separation distance between BHEs is critical in order to minimize the thermal interference between them. Although a large separation distance reduces the thermal interference, it also restricts the number of BHEs that can be installed within a given area, reducing the total length. Besides the separation distance, the BHEs must be distanced from the parcel boundaries shared with neighbouring parcels. This ensures fair use of the ground volume and minimal interference from the neighbouring systems. Dense urban areas are usually limited in space for installation of such systems. Furthermore, there are drilling restrictions usually linked to the protection of deep aquifers and presence of infrastructure such as tunnels, networks etc. [11, 9]. In Switzerland there are guidelines for the protection of ground water resources which prescribe a spatially varying maximum allowed drilling depth [12]. The above-discussed spatial constraints can greatly limit the total length that can be drilled thereby under sizing the BHEs. Therefore, a spatial modelling approach can greatly enhance the design process for installation of BHEs in urban areas. Other factors affecting heat extraction such as the spatially varying soil type can also be easily incorporated into the spatial modelling approach.

Assume an urban area consists of multiple buildings installed with BHEs extracting heat from the ground at the same time. Since the BHEs are using the same ground resource, the heat extraction of a single BHE is affected by the heat extraction of the neighbouring BHEs. Simultaneously operating BHEs in an area can cause excessive heat extraction, especially when they are under sized. Excessive heat extraction causes undesirably low temperatures in the BHE that can damage the filling material. In the worst case scenario the circulating fluid can leak and mix with the otherwise separate ground water [6, p. 28]. To prevent this, the Swiss standard for design of BHEs prescribes a minimum threshold value of -1.5^{o}C for the mean fluid temperature (MFT) in the BHE [14]. During operation, when the MFT drops below the given threshold, an auxiliary heating device is necessary to fulfil the remaining unmet heating demand of the building, until the BHE recovers naturally using the heat influx from the far ground. The heat demand that is met by the BHE maintaining the MFT above the given threshold is termed as *geothermal energy potential (GEP)*. The MFT not only depends on the short-term heat extraction from the ground but also the long-term heat extraction. Therefore, long-term operation of the BHEs can result in declining trends in the MFT over the BHEs' lifetime thereby reducing the GEP.

The above discussion highlights that the calculation of the GEP for an urban area consists of spatial as well as temporal considerations. Spatial restrictions such as parcel size, drilling depth can limit the design of BHEs that in turn can affect their operational performance. The operation of such systems over longer periods can lead to the cooling of the ground lowering the net available GEP. Emphasis must be laid on incorporating these factors into the modelling process when assessing GEP.

1.2 Previous work

Previous research suggests that there has been an increased interest in the assessment of shallow geothermal energy potential in recent years. GIS has predominantly been used to support the different methodologies proposed by several studies on this topic. The methods vary from simulation [15], analytical [9,16–18]and empirical models[15,19] to assess the GEP at relatively smaller city scales [9,20,21] as well as larger regional scales [16–18]. The purpose of these studies varies from large scale mapping [18,19,21], techno-economic decision support [16,22], CO_2 emissions mitigation [9,23], to building specific applications [9,20].

The approach by Galgaro et al. [15] employs multiple runs of a simulation model EED [24] to generate an empirical model for a BHE, to be applied to a large scale case study. They use a highly detailed description of the three-dimensional space around the BHE in terms of the ground thermal properties like thermal conductivity, diffusivity and ground temperature. The aim of this study is to generate large-scale geothermal potential maps; therefore, the detailed treatment of the BHEs, their thermal interference with each other and the specific building characteristics such as construction age, thermal insulation, heated area, occupants etc. are omitted.

Schiel et al. [9] use a specific heat extraction (sHE, Wm^{-1}) method in conjunction with a GIS based workflow to assess the shallow geothermal potential through the use of BHEs and its effects on CO_2 emissions mitigation for the city of Ludwigsburg, Germany.

This method uses the standard sHE values for each soil type which when multiplied by the total BHE length, results in the GEP. In their approach, they capture the specific building energy characteristics through energy demand calculations and spatially fitting BHEs within the parcel boundaries for each building. This building level detail is also accounted for by Zhang et al. [20] who focus on the heat pumps connected to BHEs by calculating their electricity usage and costs. They use measured COP values of GSHPs for each building. The sHE method is used in other studies such as Munoz et al. [18] to calculate the shallow geothermal potential for the large Santiago basin in Chile. They focus on BHEs as well as ground water heat exchangers (GWHEs) with depth ranging from 10-400m. Other studies for other large scale regions such as the Italian Marche [16] and south-west Germany [17] also use the sHE method for economic and technical feasibility analysis respectively. The mathematical simplicity of the sHE method and its easy integration within GIS workflows makes it favourable for the large-scale mapping of shallow geothermal potential. However, this method is incapable of accounting for spatial aspects such as thermal interference between BHEs and temporal aspects such as long-term operation, both of which affect the GEP.

Casasso and Sethi [16, 21] fill this gap by addressing the sustainable heat extraction from the BHEs over time. They follow a bottom up approach, by developing a method named G.POT that calculates the maximum possible heat extraction from each BHE by restricting the fluid temperature within the BHE to -2 °C. However, this method assumes that the BHEs respond to a single sinusoidal heat demand profile; hence, omitting the building specific details of the thermal energy demand. The method is fast and suitable for the application for large-scale mapping of the shallow geothermal potential. However, it does not address the thermal interference between BHEs that may affect their performance limiting the total geothermal potential.

A majority of the studies in the literature focus on large-scale mapping of the GEP and therefore rely on using computationally efficient methods. As a result, the bottom up modelling of the BHE systems is often not taken into consideration. The models in literature do not address the thermal interference between BHEs, long-term operational limits and their effects on the net available GEP. Although the specific characteristics that differentiate between buildings are considered in some studies, this aspect can be improved further by using state of the art building energy simulation tools.

1.3 This work

The main aim of this work is the development of a methodology to estimate the long-term GEP of an urban area focussing on (1) spatial constraints on the design of BHEs, (2) thermal interference between neighbouring BHEs (3) long-term operation of the BHEs and (4) accurate calculation of building energy demand. A GIS based workflow is developed to position and size the BHEs in an urban area taking into account drilling depth restrictions and space limitations within parcels. The methodology developed in this work considers the thermal interference of BHEs between each other. The long-term operation of the BHEs is simulated using an analytical model and its impact on the available GEP is studied. The methodology is applied to an urban neighbourhood as a case study in Switzerland. The spatial approach followed in the study can help in the planning process of large-

scale installations of BHEs in urban areas. The inclusion of the thermal interference between BHEs and their long-term operation into the modelling process provides a more accurate assessment of the GEP. The paper is organised as follows; section 2 describes the input data and developed methodology, section 3 describes the case study and its input parameters, in section 4 the main results are discussed followed by section 5 that concludes this study.

2. Methodology

The methodology developed in this study consists of three major steps: (1) calculation of thermal energy demand, (2) sizing of BHEs and (3) operation of BHEs. Furthermore, to study the effects of thermal interference between BHEs on the overall GEP a comparative analysis is made with a reference case that assumes no thermal interference between BHEs. The entire workflow has been outlined in Figure 1.

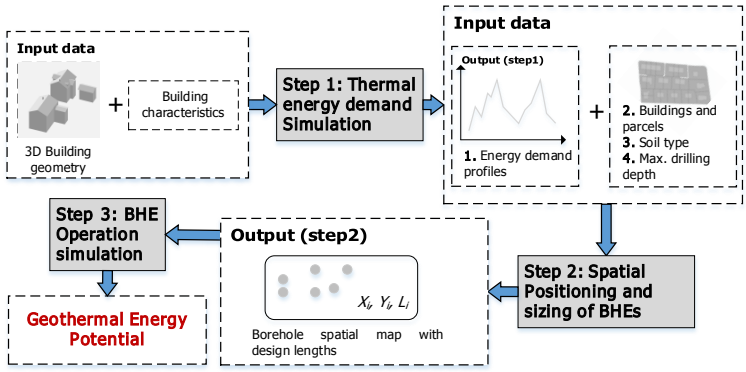

Figure 1: Overview of key steps of the methodology and their inputs and outputs

In a *first step,* total thermal energy demand for each building under consideration is calculated. Building specific characteristics such as age, thermal insulation, occupancy, glazing ratio and number of floors are taken into account. To simulate the operation of the BHEs an hourly thermal energy demand profile is necessary, therefore a dynamic building energy simulation is used as described in section 2.2.

Secondly, the BHEs are designed for each building parcel, which includes first, the spatial positioning of BHEs within the building's parcel and second, sizing the BHEs for their total length to satisfy the given thermal energy demand. A GIS based workflow is used as described in section 2.3.

Thirdly, an analytical model accounting for the thermal interference between BHEs is used to simulate the long-term operation of the BHEs. Hourly thermal energy demand is used as input for the simulation. The time varying MFT is obtained and is used to calculate the unmet heat demand. This is described in section 2.4.

As a result, the long-term annual potential of geothermal energy is calculated through aggregation of the met heating demand as described in section 4.6.

Subsequently, a comparative analysis is performed to emphasize the impact of thermal interference between BHEs. The results of this study are compared with a reference case that assumes no thermal interference between BHEs as described in section 4.5.

2.1 Input Data

The main input data used for building energy simulation are the 3D building geometry, weather data and building specific characteristics. GIS data on building footprints, parcel boundaries, soil type and drilling restrictions (Figure 2) is used in the modelling of the GEP. A list of the main input data used along with their source and technical specifications are summarized in table 1.

Table 1: Input data: description, technical information and source

Dataset	Format	Description	Source
Building Geometry	CAD dxf file format	3D CAD model of each building	Swisstopo [26]
Building characteristics	Points (Esri Shapefile)	Building characteristics such as, age, number of floors, occupants. Each building is represented by a point.	Bundesamt für Statistik [27]
Weather data	Energy Plus epw file format	Energy plus weather file interpolated using Meteonorm [28]	Meteonorm [28]
Building footprints	Polygon (ESRI Shapefile)	The building footprints from the municipality cadastre data as a polygon vector file.	Amt für Raumentwicklung (ARE) [29].
Parcel boundaries	Polygon (ESRI Shapefile)	The parcel boundaries from the municipality cadastre data as a polygon vector file.	ARE [29]
Soil type	Polygon (ESRI Shapefile)	The spatial distribution of soil type as a polygon vector file. The thermal properties for each soil type are derived from [14]	Federal Office of the Environment [30]
Maximum drilling depth	Raster	The maximum allowed drilling depth as a raster with a 5m resolution (*Figure 2*). This dataset is based on the water protection law [12]	ARE [31]

2.2 Thermal energy demand simulation

The thermal energy demand of each building consisting of space heating, cooling and DHW is calculated on an hourly basis using an approach developed by Wang et al. [32]. The input data used for this calculation are the building geometry in the form of a 3D CAD model, the building specific characteristics including building age, glazing ratio, number of floors, occupants and the local weather conditions in the form of a typical meteorological year (TMY) weather file. This approach uses Energy Plus [33], a dynamic building energy simulation program that accounts for occupancy schedules, thermostat settings, infiltration rates etc. for each building separately. The 3D geometry of each building is used to calculate thermal zones within the building as well as shading effects from the surrounding buildings that influences the solar gains. As a result, hourly profiles for space heating, cooling and DHW demand for each building are obtained for the whole year. Since the building is coupled to the BHE through a heat pump, a constant COP of 4.0 and EER of 4.5 is assumed for the heat pump to calculate the ground loads. In practice, the COP and EER varies with BHE temperature, load side delivery temperature, load/source side mass flow rates etc. Since the heat pump is not central to this study constant values have been assumed.

2.3 Design of BHEs

The design of BHEs is divided into two parts, *first*, the spatial positioning of BHEs within the building parcel and *second*, the sizing of the BHEs to satisfy the given heat demand.

2.3.1 Spatial positioning of BHEs

A GIS based workflow is developed to calculate the area eligible for the installation of BHEs for each building parcel. The placement of the BHEs within the parcel must obey spatial constraints including, a minimum separation distance of 5m between BHEs as prescribed by the Swiss standard for design of BHEs [14]. A conservative value of 7.5m is chosen for this study to minimise thermal interference between BHEs as compared to the case with separation distance of 5m. A safety margin of 3m is maintained inwards from the parcel boundary and outwards from the building wall where no BHEs can be installed. This margin is subtracted from the total parcel area to get the eligible area. Figure 3 demonstrates the eligible area for a selection of example buildings. In the next step, a regular matrix of points, each representing a BHE, is fit into the eligible area polygon obtained in the previous step. Finally, GIS data on maximum allowed drilling depth and local soil type is extracted for each point from the data layers described in Table 1 and added as attributes. A spatial map of BHEs each represented by a point with fixed coordinates having soil type and drilling depth as attributes is obtained.

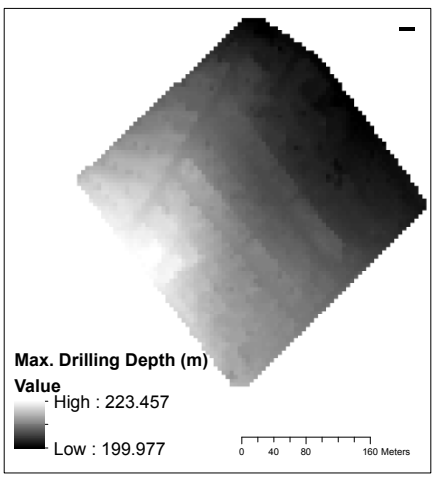

Figure 2: Maximum drilling depth (in m) raster for the case study

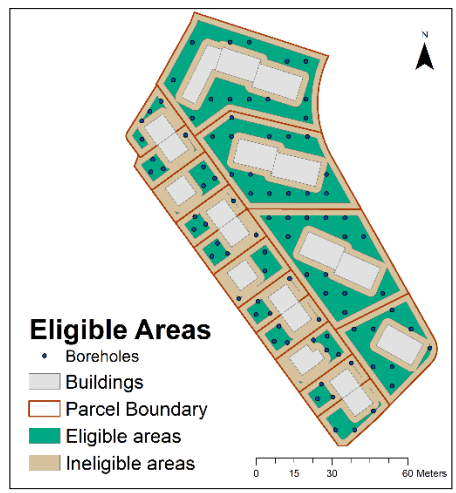

Figure 3: Eligible area around buildings for installation of BHEs

2.3.2 Sizing the BHE length

The ASHRAE method [34], further simplified by Bernier [35] is used for calculating the design length of the BHEs and the main equation used for this calculation is given by (1). Calculations are performed only for the heating cycle, as it is the predominant mode of operation for the case study described in section 3.

$$L_h = \frac{q_h R_b + q_y R_{10y} + q_m R_{1m} + q_h R_{6h}}{T_{mf} - (T_{gr,\infty} + T_p)} \tag{1}$$

Where L_h is the BHE design length for the heating cycle. q_h, q_y, q_m are respectively the peak hourly, yearly average and peak monthly ground loads in W. R_b, R_{10y}, R_{1m} and R_{6h} are respectively the borehole thermal resistance, effective ground thermal resistances for a 10 yearly, monthly and 6 hourly pulse in mK/W. T_{mf}, $T_{gr,\infty}$ and T_p are respectively the MFT in the BHE u-pipe,

the undisturbed ground temperature and the temperature penalty in K. The detailed calculation methods for effective thermal resistances of the ground for different thermal pulses are described by Kavanaugh & Rafferty [34].

T_p, the temperature penalty represents the average ground cooling at the end of the lifetime of the BHE, allowing including the effects of ground cooling into the design process. To estimate T_p a method prescribed by ASHRAE is used [34]. This method is based on the calculation of the ground volume around a BHE in which the annual heat imbalance is stored. If there is an annual net heat extraction, the temperature of this volume decreases and vice versa. An energy balance assuming steady state is used to calculate this change in temperature of the given volume at the end of the BHE's lifetime. In the next step, an iterative procedure is followed which updates the temperature penalty after each calculation of the length until it converges and results in the final design length.

2.4 BHE operation simulation

Once the design of the BHEs is successfully achieved and their spatial positions and lengths are fixed, the operation of the BHEs is simulated using a mathematical model. This simulation is performed for each BHE on an hourly basis for 10 years. A value of 10 years is chosen to keep the simulation computationally tractable. First, the borehole map consisting of X_i, Y_i coordinates and lengths (L_i) obtained from the design process are used as input to calculate the thermal response factors (g-functions, see section 2.4.1). Temporal superposition is applied to all the BHEs using their g-functions and heat demands to obtain their respective temperature responses (see section 2.4.2). Spatial superposition is applied to calculate the BHE wall temperature accounting for thermal interference from neighbouring BHEs. Subsequently, a steady state heat transfer equation is used to calculate the time varying MFT. The different parts of the workflow used for the mathematical modelling of the operation are described in the following sections and summarized in Figure 4.

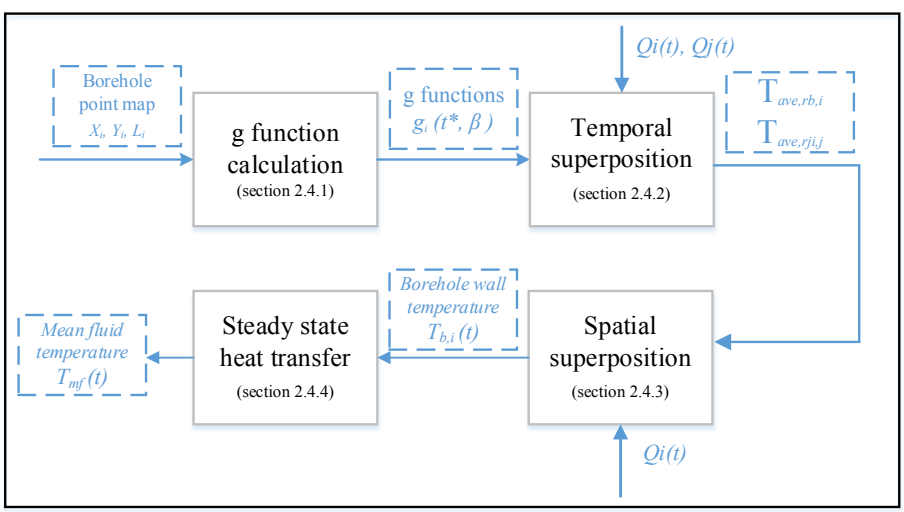

Figure 4: Workflow describing the modelling of the BHE operation simulation

2.4.1 BHE Thermal response

g-functions

g-functions also called as dimensionless temperature response factors were first described and defined in Eskilson's PhD thesis [36]. They enable the quantification of the average temperature over BHE length at any radius around a BHE, in response to a step heat pulse. The g-functions are calculated as the solution to the finite line source (FLS) model [37] of the BHEs. A numerically efficient analytical expression given by (2) developed by Lamarche & Beauchamp [38] for the FLS solution is employed to calculate the g-function for each BHE.

$$g(t^*, \beta) = \int_{\beta}^{\sqrt{\beta^2+1}} \frac{erfc(\gamma z)}{\sqrt{z^2-\beta^2}} dz - D_A - \int_{\sqrt{\beta^2+1}}^{\sqrt{\beta^2+4}} \frac{erfc(\gamma z)}{\sqrt{z^2-\beta^2}} dz - D_B \quad (2)$$

$$\beta = \frac{r}{L}; \qquad t^* = \frac{t}{t_s}; \qquad t_s = \frac{L^2}{9\alpha}$$

Where r is the radial distance from the BHE center; L is the BHE length; t is the time and α is the thermal diffusivity of the ground surrounding the BHE. D_A and D_B are functions dependent on time and BHE length the detailed definition of which can be found in [38].

Temperature response

According to the definition of g-functions, (3) is used to obtain the actual temperature response from its non-dimensional form. The actual temperature response i.e. the average temperature at given radius from the BHE centre is dependent on the thermal properties of the ground surrounding the BHE, its length and the step heat pulse applied to the ground.

$$T_{ave,r} - T_{gr,\infty} = \frac{Q}{2\pi kL} g\left(\frac{t}{t_s}, \frac{r}{L}, BHE\ coordinates\right) \quad (3)$$

Where $T_{ave,r}$ is the temperature at the distance r from the borehole averaged over the BHE length, $Q(t)$ is the step heat pulse acting on the borehole, k is the thermal conductivity of the ground, L is the BHE length, r is the radial distance from the BHE centre, t is time, g is the g-function.

2.4.2 Temporal superposition

The g-functions by definition enable the calculation of the temperature response of a BHE only to a *step heat pulse*. In practice, the heating demand varies over time, which makes it necessary to convert the time varying profile into the temporal superposition of several step heat pulses. This is done using (4) and the detailed algorithmic flow is described in [41].

$$T_b(t_n) - T_{gr,\infty} = \sum_{i=1}^{n} \frac{(Q_i - Q_{i-1})}{2\pi kL} g\left(\frac{t_n - t_{i-1}}{t_s}, \frac{r_b}{L}\right) \quad (4)$$

Where Q_i is the heat pulse for time step t_i ∀ i ∈ (1, n); n is the total number of heat pulses; r_b is the radius of the BHE boundary wall and T_b is the temperature at the BHE boundary wall. This calculation is performed for each of the time instant (t_n) to create a smooth hourly evolution curve of T_b.

To improve computational times for simulation of long-term BHE operation, aggregation of loads is carried out. Several approaches have been used in the literature for the aggregation of loads including the multiple load aggregation algorithm (MLAA) [42] and the simple algorithm proposed by Yavuzturk and Spitler [41]. The latter is employed in this study. The conceptual basis of this algorithm is to lump the loads that have occurred more than a given time ago into blocks of a given size. The given time is specified as an input parameter called the minimum hourly history period (MHHP), and the given size is specified as the aggregated load block (ALB). A value of 192h for the MHHP is sufficient to keep the error in final temperatures due to aggregation within ±0.05°C [41]. In this study, conservative value of 500h for MHHP and additionally a value of 730h for ALB has been used.

2.4.3 Spatial superposition

The thermal interference between BHEs is accounted for using the superposition principle [38, 39]. It states that thermal response of given BHE is equal to the superposition of the respective thermal responses of neighbouring BHEs, each calculated at the centre of the given BHE. The superposition principle can be written in terms of temperature response as described by (5).

$$T_{ave,r_b,i} = T_{ave,r_b,i}\big|_{g_i(r=r_b,\,t),\ Q_i} + \sum_{\forall j \neq i} T_{ave,r_{ji},j}\big|_{g_j(r=r_{ji},\,t),\ Q_j} \tag{5}$$

Where T_i is the net temperature response of the ith BHE due to itself and neighbouring BHEs. $T_i|_{g_i(r=r_b,\,t),\ Q_i}$ is the temperature response of the ith BHE calculated at $r = r_b$ and heat pulse Q_i. $T_j|_{g_j(r=r_{ji},\,t),\ Q_j}$ is the temperature response of the jth neighbour calculated at a distance $r = r_{ji}$ and heat pulse Q_j. r_{ji} is the distance from the jth BHE to the ith BHE.

2.4.4 Mean fluid temperature (MFT)

The MFT can be calculated by assuming steady state heat transfer between the heat carrier fluid in the u-pipe and the borehole boundary wall. The borehole is filled with grout material that acts as a thermal resistance between the u-pipe containing the thermal carrier fluid and the surrounding ground. For the sake of simplicity, a constant value 0.17 is assumed for the grout thermal resistance R_b. MFT is calculated using (6).

$$T_{mf}(t) = T_b(t) - \frac{Q(t)\,R_b}{L} \tag{6}$$

Where$T_{mf}(t)$, is the MFT in the u-pipe, $Q(t)$ is the net thermal energy exchanged from the given BHE both as functions of time and L is the length of the given BHE. The MFT in all BHEs is restricted above -1.5°C that could result in a part of the heat demand being unmet. Since there are no upper limits to the MFT, the cooling demand is always met.

2.5 Geothermal Energy Potential (GEP)

The heating demand of the buildings that is met by the BHEs maintaining the TMF above the restrictive threshold of -1.5°C is aggregated for the whole year to calculate the GEP.

3. Case Study

3.1 Description

In order to illustrate the methodology developed in this study, a neighbourhood called Altstetten, in Zurich, Switzerland is chosen as a case study. It consists of 170 buildings confined within 135 parcels spanning an area of 108,000 m^2. All the buildings are residential with a mix of detached single-family houses, semi-detached family houses, terraced/row houses and small medium and large multi-family apartments as shown in Figure 5. The use of GSHPs is suggested by the city of Zurich in their energy plan for 2050 as centralized solutions such as district heating are not ideal due to its low energy density [43]. This is illustrated by figure 6. The area spanned by the case study is divided into two soil type zones, first of which covers almost 85% of the area consists of silt and clay (zone1), and the second, which consists of loamy gravel (zone2).

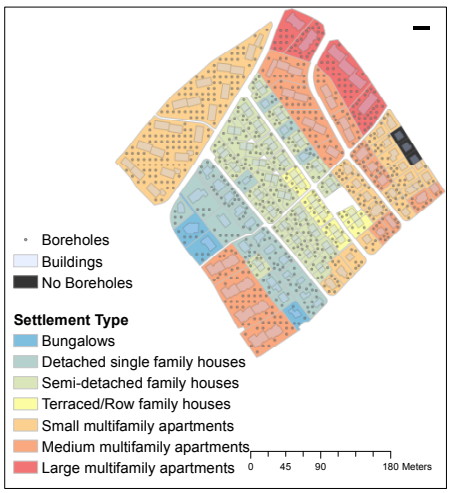

Figure 5: Settlement types within the case study

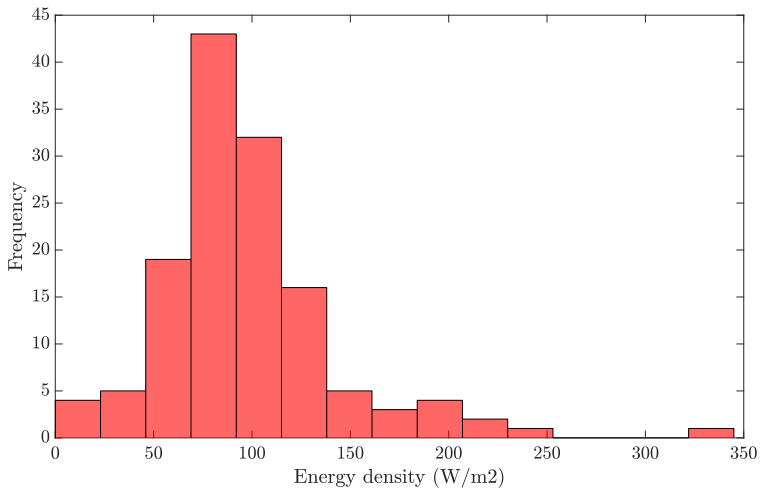

Figure 6: Distribution of energy density of parcels within the case study

3.2 Input parameters

Table 2 lists the input parameters for the case study with their respective values, units and the source for their values.

Table 2: Input parameters for the case study

Parameter	Unit	Value	Source
Borehole separation	m	7.5	Chosen value recommended by SIA [14
Buffer distance from building/parcel boundaries	m	3	Chosen value
Design MFT	°C	-1.5	SIA design standard [14]
Coefficient of performance (COP)	-	4	Chosen value
Energy Efficiency Ratio (EER)	-	4.5	Chosen value
Borehole thermal resistance	m K/W	0.17	ASHRAE Handbook [34]
Borehole diameter	mm	125	ASHRAE Handbook [34]
Pipe diameter	mm	32	ASHRAE Handbook [34]
Soil thermal conductivity	W/m K	1.7 (zone1), 1.4 (zone2)	SIA design standard [14]
Soil thermal diffusivity	m2/day	0.063 (zone1), 0.052(zone2)	SIA design standard [14]
BHE system lifetime	Years	50	Chosen value
ALB	Hours	730	Chosen value
MHHP	Hours	500	Chosen value

4. Results and Discussion

4.1 Heat energy demand

The spatial distribution of the annual heat demand (kWh/m^2/a) which includes space heating and DHW, calculated per parcel, is shown in Figure 7a. The peak heat demand is shown in Figure 7b. The annual heat demand ranges from 53 to 330 kW/m^2/a. It is the highest for parcels with relatively old single-family detached, semi/detached and row houses and the lowest for parcels containing newly built multifamily houses. The peak heat demand ranges from 13 to 410 kW. It is higher for the larger parcels with multifamily houses and lower for the smaller parcels consisting of single-family houses.

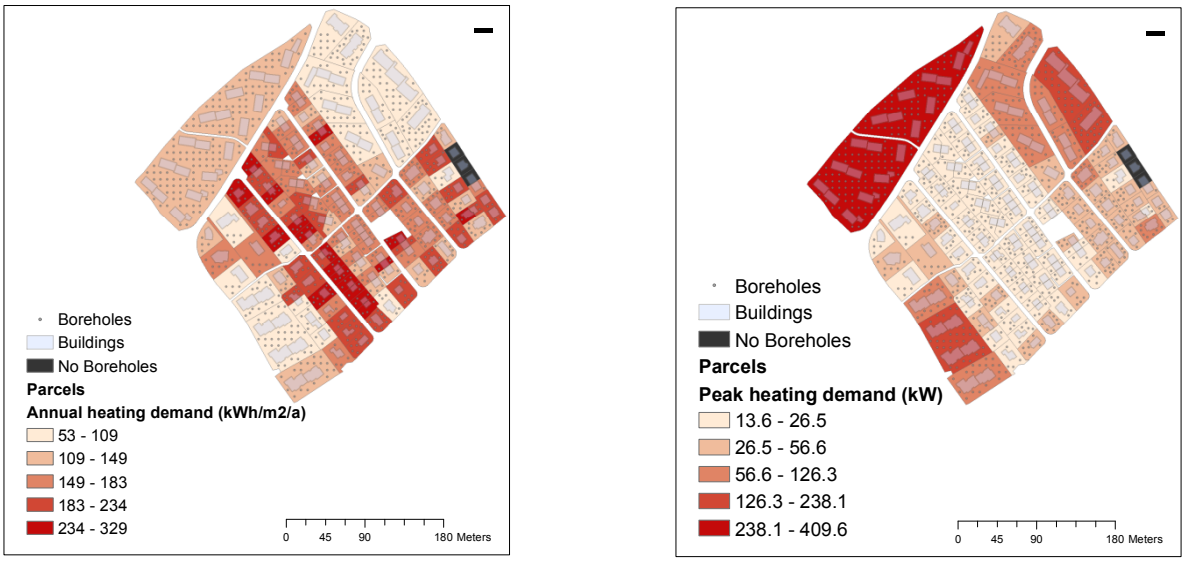

(a) Annual heating demand (kWh/m^2/a) (b) Peak heating demand (kW)

Figure 7: Heating demand for DHW and space heating

Additionally, the observed departure from the above-mentioned general trends and other smaller variation between distinct buildings can be attributed to factors such as variations in occupancy profile, thermostat usage, glazing ratios, attachment to other buildings, and shading from neighbouring buildings.

4.2 BHE design

Figure 8a shows average BHE design length (m) per parcel taking into account the drilling constraints. The BHE length ranges from 180m to 220m that are typical for such systems. A spatial correlation of the BHE length with the maximum allowed drilling depth is observed. This is due to the under sizing of BHEs as the result of the presence of drilling depth restrictions. The required length for supplying the heat energy demand for almost all parcels is greater than the maximum drilling depth, causing the BHEs to be under sized. This is illustrated in Figure 8b that depicts the BHE length as a percentage of total required length. It is observed that the BHE design length is as low as 15% of the required length leaving the BHE 85% under sized. There are three

parcels highlighted in Figure 8b (black) where no boreholes can fit due to spatial restrictions such as parcel boundary being too close to the building boundary.

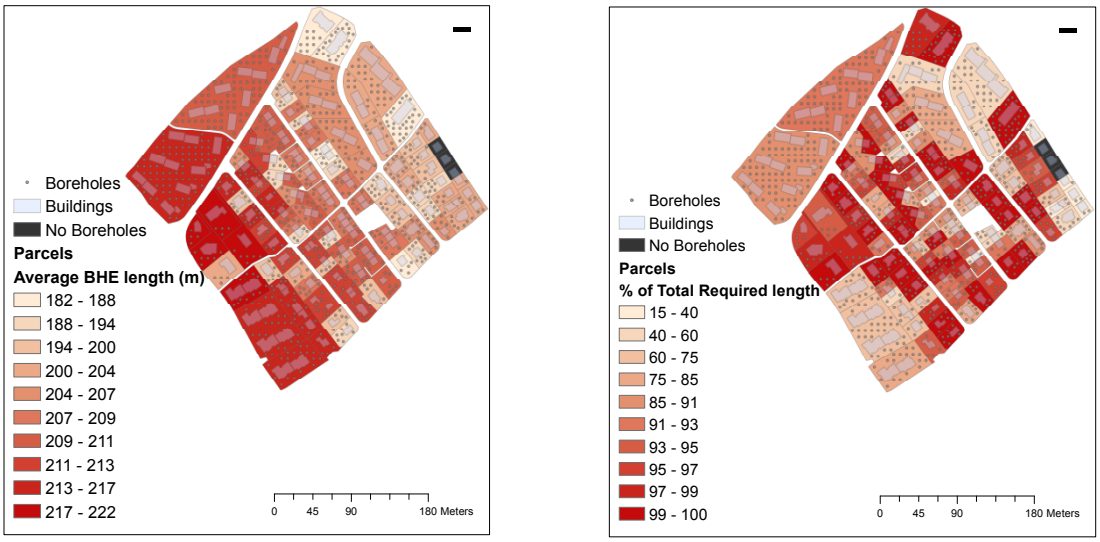

(a) Average BHE length per parcel (m) (b) Percentage of total required length

Figure 8: BHE design lengths

4.3 BHE Operation

The MFT is restricted above a threshold of -1.5°C. As it drops below this given threshold, the operation of the BHE is interrupted and heating demand is unmet. This is illustrated in Figure 9 that shows the hourly met and unmet heat demand of a single example BHE in parallel with the hourly evolution of the MFT within the BHE for first year of operation. It is clear that some of the heating demand remains unmet by the BHE system hence the need for auxiliary heating technologies is necessitated. This will help in achieving security of heat supply for the building. This unmet heating demand can be attributed to insufficient length of the BHE and/or the simultaneous heat extraction of multiple BHE systems in close vicinity.

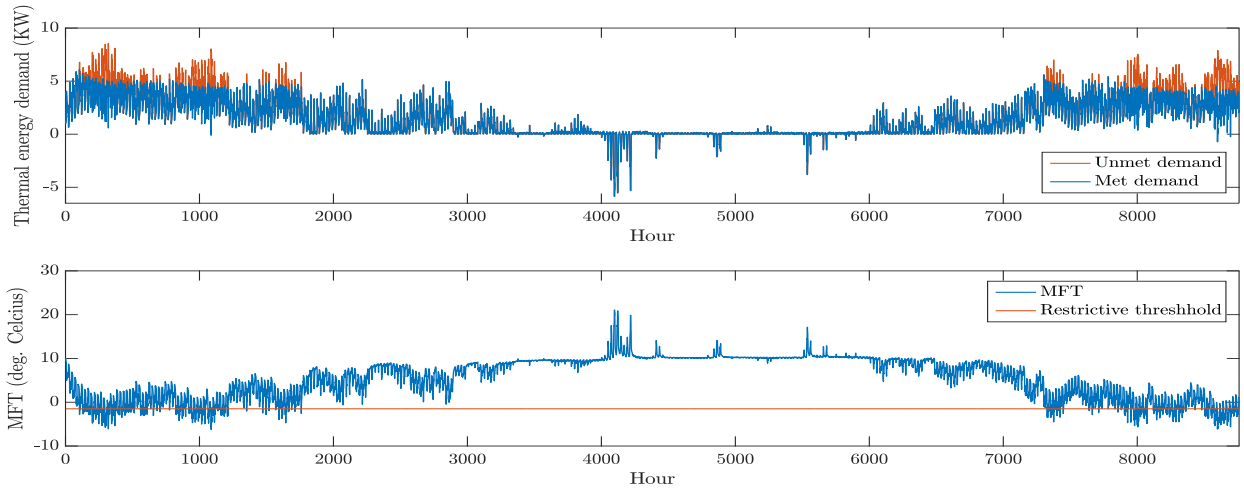

Figure 9: Hourly heating/cooling demand and MFT variation for a single example BHE in the 1st year of operation

Figure 10a shows the maximum number of hours of unmet heat demand per parcel in the 1st year of operation. A majority of parcels have minor interruption of the BHE operation within the range of 0-25 unmet hours annually and some have major interruptions going upto 2500 to 4000 unmet hours. The interruption of BHE operation does not necessarily imply the total failure in the supply of the heat demand to the building. In case of interruption, the unmet heat demand can be met through auxilliary technologies such as a gas boiler. The unmet heat demand (percentage of total) for each parcel is shown in Figure 10b. Its highest value is within 10% of the total heat energy demand. However, these results are only the first year of operation. The long-term operation of the BHEs increases the percentage of unmet heat demand over time. This long term effect is illustrated by Figure 11a,b as described below.

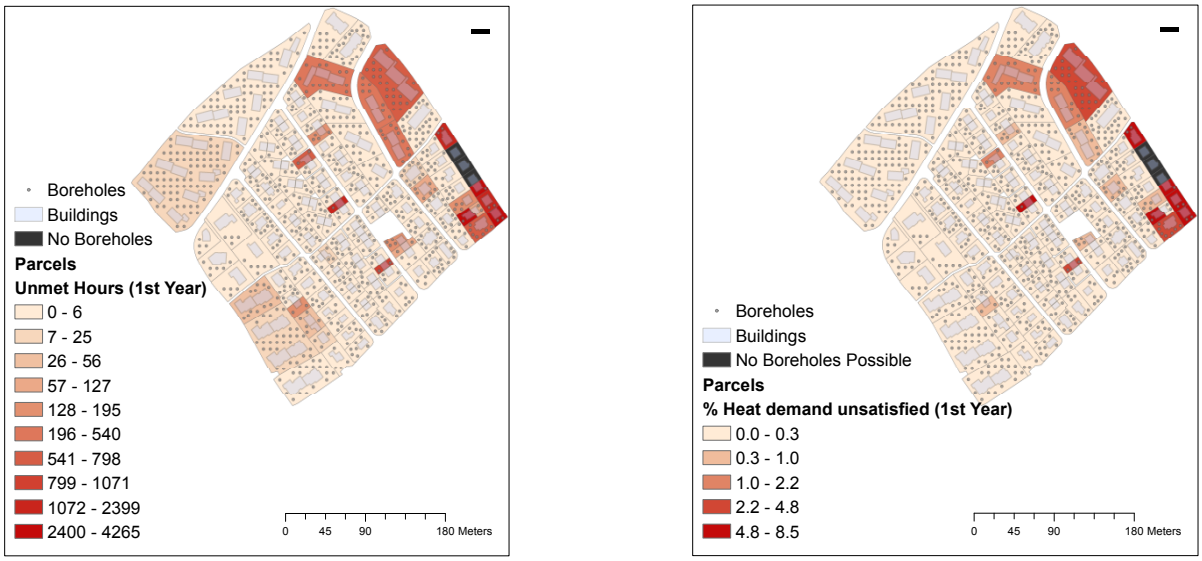

(a) Hours of unmet demand per parcel (b) Percentage heat demand unmet

Figure 10: BHE interruption of operation in the first year

4.4 Long term operation

Figure 11a shows the distribution of the number of unmet hours for each parcel (represented by dots) over 10 simulated years of operation. It is observed that the mean number of unmet hours increases at a slow rate up until the 5th year of operation followed by a steep increase in the later years of operation. The spread of values also increases with time indicating the time dependent behaviour of each BHE within each parcel depending upon its specific heating demand, spatial location, influence from neighbours etc. There are several parcels which, starting from the first year of operation itself exhibit a high number of unmet hours. These unmet hours in most cases, occur during the heating season and hence any value above a few hundred hours is a serious cause for concern in the viability of such systems. This can be solved through interventions in the building's energy supply system such as using gas boilers for supplying peak heat demand and solar thermal collectors for seasonal regeneration of the ground. Demand side interventions such as retrofit of the building envelope can reduce the heat demand of the building thereby reducing the load on the BHEs. Figure 11b similarly shows the distribution of unmet heating demand relative to the total heating demand for each

parcel. Similar trends are observed and it is clear that on an average the amount of unmet heating demand is almost zero up until the 7th year of operation. There are parcels which require heat to be put into ground to maintain adequate temperatures in the BHE for smooth operation (values > 1) starting as early as the first year of operation. The short and long-term variation in the MFT for an example BHE are shown in Figure 12. Cases with and without restriction of the MFT above -1.5°C are displayed. A BHE in which the long-term effects are more pronounced is selected. It indicates a declining trend over time as heat is continuously extracted each year. This causes the number of unmet hours and unmet heat demand to increase with each year of operation. The unmet heat demand can be reduced or eliminated if the net annual heat imbalance is close or equal to zero. Therefore, in areas where heat extraction during winter is predominant, excess heat can be added to the ground during the summer season for instance, using solar thermal systems.

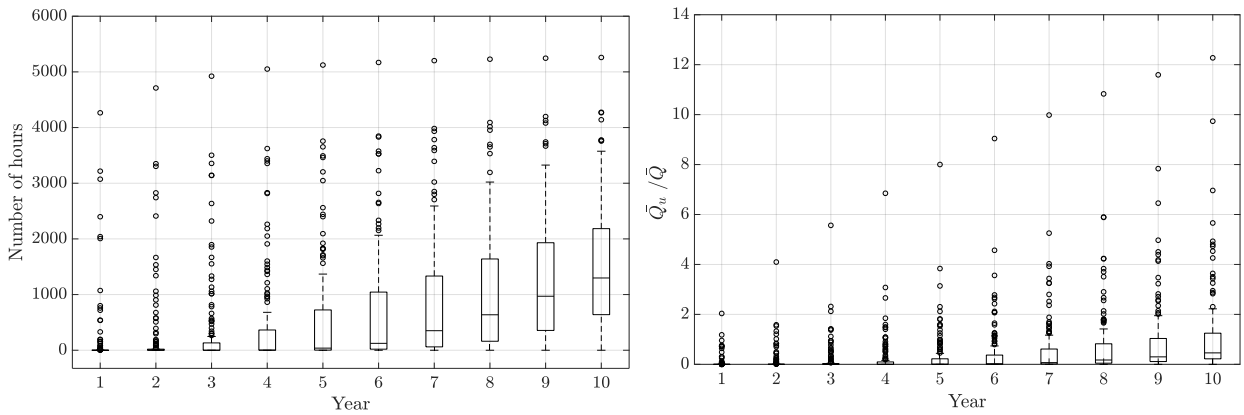

(a) (b)

Figure 11: Distribution of hours of (a) interrupted operation and (b) heat demand for all parcels over 10 years of operation

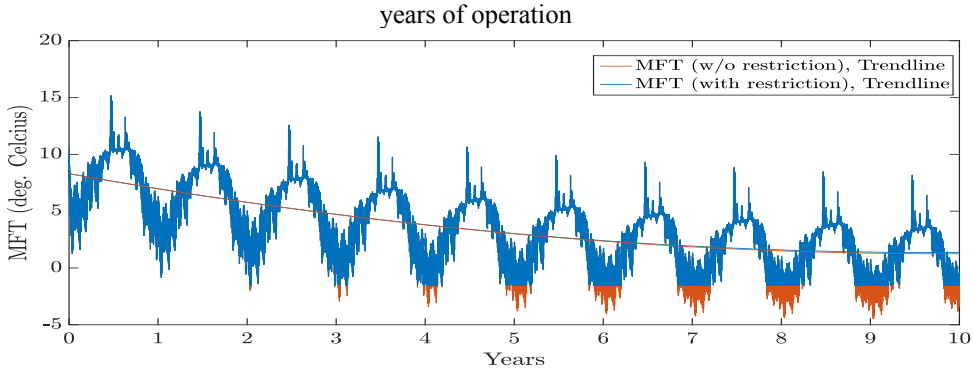

Figure 12: Long-term variation and trends in the MFT for an example BHE

4.5 Impact of thermal interference

To emphasize the impact of thermal interference between BHEs on each other's thermal performance and thereby the GEP, a comparative analysis is performed. The results of this study are compared to a reference case that assumes no thermal interference between BHEs. Figure 13 shows the long-term variation and trends in the MFT for the same example BHE now for the reference case. The MFT with and without restriction above -1.5°C and hence the trend lines follow the same path since the MFT does not

cross this threshhold. The MFT exhibits a very small overall cooling trend but it is less pronounced as observed in Figure 12. The MFT does not cross the restrictive threshold providing uninterrupted BHE operation. This indicates that the BHEs appear to operate without any interruption and without any significant overall cooling of the ground over long period.

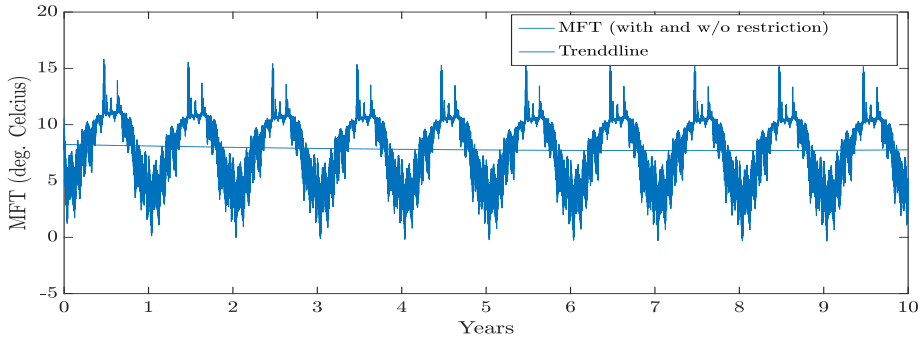

Figure 13: Long-term variation and trends in the MFT for the same example BHE for the reference case (no interference)

The results of the unmet heat demand for the reference case are described in Figure 14. On an average, most of the parcels have almost zero number of hours of interrupted operation even up until the 10th year of operation. Similarly, the ratio of unmet heat demand to the total heat demand for most parcels remain close to zero also up until the 10th year of operation. This indicates that for most parcels a long term uninterrupted operation is possible if thermal interference between BHEs did not exist. Although there are some parcels that are outliers to this effect that can be attributed to the insufficient lengths of their BHEs. Furthermore, the magnitude by which they lie outside is lower if compared to Figure 11. This indicates that the overall GEP is overestimated if thermal interference between BHEs is not considered in the modelling proces. It can be concluded through this comparative analysis that for an accurate calculation of the long term GEP for an urban area, thermal interference between BHEs should be taken into account in the model.

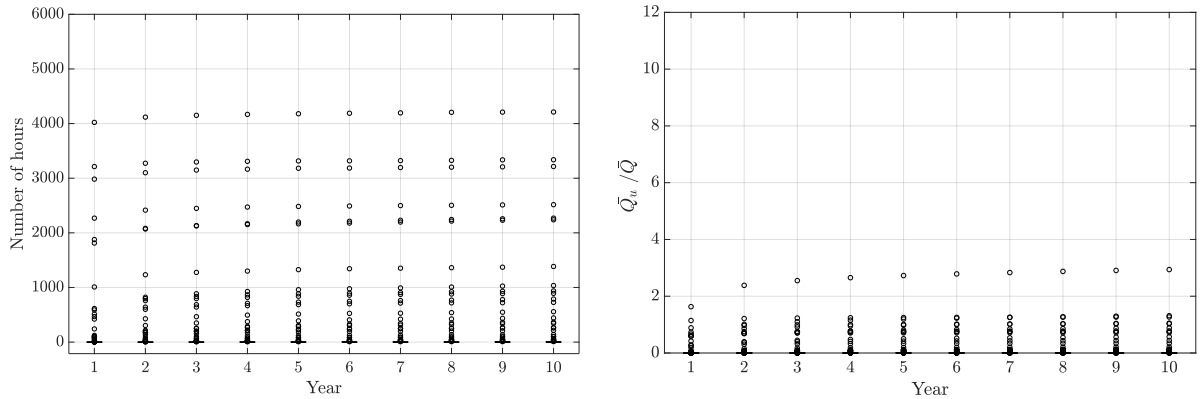

(a) (b)

Figure 14: Distribution of hours of interrupted operation (a) and heat demand (b) for parcels over 10 years of operation for reference case (no interference)

4.6 Geothermal Energy Potential

Figure 15 shows the evolution of of the net GEP normalized by the parcel area (in W/m2) for all the parcels for 10 years of operation. On an average the trends show that there is a decrease in the net GEP for majority of the parcels over time which can be attributed to ground cooling. Parcels with relatively high energy density exhibit a sharper decline in the net GEP whereas the parcels with low energy density exhibit a slow decline. This is due to the limited heat capacity of the ground and overuse. Auxilliary systems like gas boiler, solar thermal collectors can be used to limit the overuse of the ground. This can help maintain the sustainabilits of the GEP.

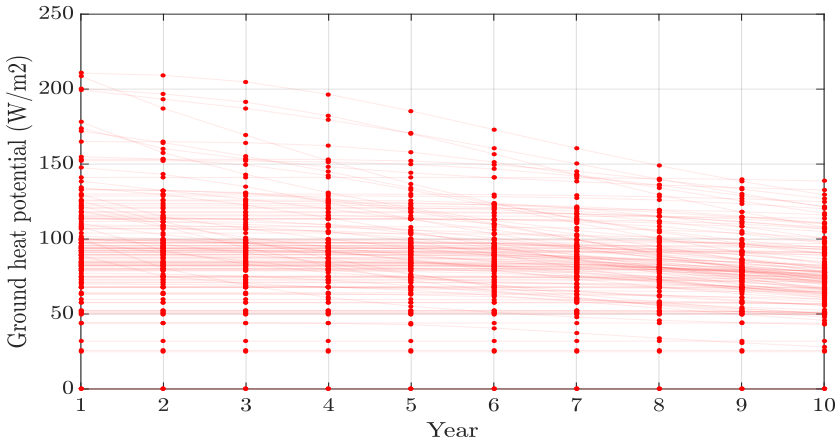

Figure 15: GEP per unit parcel area for all parcel over 10 years of operation

5. Conclusion

In this study, a GIS based methodology is developed to estimate the sustainable GEP in an urban area where multiple buildings are equipped with BHEs in conjunction with GSHPs. The developed methodology addresses the practical constraints in the design and operation of GSHPs and their effects on the net available GEP and its sustainability over longer periods. A GIS based workflow is developed to position and size the BHEs taking into account drilling depth restrictions and spatial variation of soil type. Thermal interference between BHEs is also accounted for and its effects of the net available GEP are studied. This method is subsequently applied to an urban neighbourhood called Altstetten in Zurich, Switzerland as a case study. The results indicate that due to the limitations in the drilling depths in urban areas, the BHEs are undersized limiting the amount of thermal energy that can be exchanged with the ground. This necessitates the evaluation of the BHEs operational performance that affects the net GEP. The BHEs in the entire urban area are operating simultaneously and have a significant impact on each other's thermal performance. This is illustrated through comparing the developed methodology to a reference case that assumes no thermal interference between BHEs. It has been shown that the GEP is overestimated if thermal interference is not taken into account. There are several hours in the heating season when the heat pump operation is interrupted necessitating the use of backup auxiliary technologies to fulfil the unmet heat demand. The magnitude of the unmet demand depends on how long the system has been

operating and exchanging heat with the ground. The results also show that the GEP decreases over longer periods of heat extraction. This can be addressed through the thermal regeneration of the ground. Technologies such as solar thermal collectors can be used to recharge the ground during the summer season, boilers based on natural gas or oil may well be used. The design of the technical systems to recharge the ground and simultaneously provide a secure thermal energy supply to the buildings is a matter of future scientific enquiry.

Acknowledgements

This research in the present contribution was funded in part by SCCER "Future Energy Efficient Buildings and Districts" (CTI.1155000149).

References

[1] Europe 2020: A strategy for smart, sustainable and inclusive growth, Brussels, 2010. doi:10.1007/s13398-014-0173-7.2.

[2] Energy Roadmap 2050, Brussels, 2011.

[3] International Energy Agency, Transition to Sustainable Buildings - Strategies and opportunities to 2050, Paris, 2013. doi:10.1787/9789264202955-en.

[4] J.O. Lewis, S.N. Hógáin, A. Borghi, Building Energy Efficiency in European Cities, Paris, 2013. http://urbact.eu/fileadmin/general_library/19765_Urbact_WS6_ENERGY_low_FINAL.pdf.

[5] Directive 2010/31/EU of the European Parliament and of the Council of 19 May 2010 on the energy performance of buildings (recast), Brussels, 2010. doi:doi:10.3000/17252555.L_2010.153.eng.

[6] C. Karytsas, Current state of the art of geothermal heat pumps as applied to buildings, Adv. Build. Energy Res. 6 (2012) 119–140. doi:10.1080/17512549.2012.672004.

[7] I. Sarbu, C. Sebarchievici, General review of ground-source heat pump systems for heating and cooling of buildings, Energy Build. 70 (2014) 441–454. doi:10.1016/j.enbuild.2013.11.068.

[8] G. Florides, S. Kalogirou, Ground heat exchangers-A review of systems, models and applications, Renew. Energy. 32 (2007) 2461–2478. doi:10.1016/j.renene.2006.12.014.

[9] K. Schiel, O. Baume, G. Caruso, U. Leopold, GIS-based modelling of shallow geothermal energy potential for CO2 emission mitigation in urban areas, Renew. Energy. 86 (2016) 1023–1036. doi:10.1016/j.renene.2015.09.017.

[10] R.H.D. Rawlings, J.R. Sykulski, Ground source heat pumps: A technology review, Build. Serv. Eng. Res. Technol. 20 (1999) 119–129. doi:10.1177/014362449902000304.

[11] S. Haehnlein, P. Bayer, P. Blum, International legal status of the use of shallow geothermal energy, Renew. Sustain. Energy Rev. 14 (2010) 2611–2625. doi:10.1016/j.rser.2010.07.069.

[12] A. Amt fur Abfall, Wasser, Energie und Luft, Energienutzung aus Untergrund und Grundwasser, Zurich, 2010.

[13] E. Bertram, Heat Pump Systems with Vertical Ground Heat Exchanger and Uncovered Solar Thermal Collectors, MV-Verlag, 2015.

[14] Schweizerischer Ingenieur- und Architektenverein, Erdwärmesonden. SIA 384/6:2010, Zurich, 2010.

[15] A. Galgaro, E. Di Sipio, G. Teza, E. Destro, M. De Carli, S. Chiesa, A. Zarrella, G. Emmi, A. Manzella, Empirical modeling of maps of geo-exchange potential for shallow geothermal energy at regional scale, Geothermics. 57 (2015) 173–184. doi:10.1016/j.geothermics.2015.06.017.

[16] A. Gemelli, A. Mancini, S. Longhi, GIS-based energy-economic model of low temperature geothermal resources: A case study in the Italian Marche region, Renew. Energy. 36 (2011) 2474–2483. doi:10.1016/j.renene.2011.02.014.

[17] J. Ondreka, M.I. Ruesgen, I. Stober, K. Czurda, GIS-supported mapping of shallow geothermal potential of representative areas in south-western Germany-Possibilities and limitations, Renew. Energy. 32 (2007) 2186–2200. doi:10.1016/j.renene.2006.11.009.

[18] M. Muñoz, P. Garat, V. Flores-Aqueveque, G. Vargas, S. Rebolledo, S. Sepúlveda, L. Daniele, D. Morata, M.Á. Parada, Estimating low-enthalpy geothermal energy potential for district heating in Santiago basin–Chile (33.5 °S), Renew. Energy. 76 (2015) 186–195. doi:10.1016/j.renene.2014.11.019.

[19] A. Casasso, R. Sethi, G.POT: A quantitative method for the assessment and mapping of the shallow geothermal potential, Energy. 106 (2016) 765–773. doi:10.1016/j.energy.2016.03.091.

[20] Y. Zhang, R. Choudhary, K. Soga, Influence of GSHP system design parameters on the geothermal application capacity and electricity consumption at city-scale for Westminster, London, Energy Build. 106 (2015) 3–12. doi:10.1016/j.enbuild.2015.07.065.

[21] A. García-Gil, E. Vázquez-Suñe, M.M. Alcaraz, A.S. Juan, J.Á. Sánchez-Navarro, M. Montlleó, G. Rodríguez, J. Lao, GIS-supported mapping of low-temperature geothermal potential taking groundwater flow into account, Renew. Energy. 77 (2015) 268–278. doi:10.1016/j.renene.2014.11.096.

[22] P. Blum, G. Campillo, T. Kölbel, Techno-economic and spatial analysis of vertical ground source heat pump systems in Germany, Energy. 36 (2011) 3002–3011. doi:10.1016/j.energy.2011.02.044.

[23] P. Blum, G. Campillo, W. Münch, T. Kölbel, CO2 savings of ground source heat pump systems – A regional analysis, Renew. Energy. 35 (2010) 122–127. doi:10.1016/j.renene.2009.03.034.

[24] P. Eskilson, G. Hellstrom, J. Claesson, T. Blomberg, B. Sanner, Earth Energy Designer (EED), Lund, Sweden, 2000. http://www.buildingphysics.com/manuals/eed.pdf.

[25] A. Casasso, R. Sethi, Assessment and mapping of the shallow geothermal potential in the province of Cuneo (Piedmont, NW Italy), Renew. Energy. (2016). doi:10.1016/j.renene.2016.10.045.

[26] Swiss Federal Office of Topography, swissBUILDINGS3D, Zurich, 2013.

[27]Bundesamt für Statistik, Gebäude- und Wohnungsregister, Zurich, 2013. https://www.bfs.admin.ch/bfs/de/home/register/gebaeude-wohnungsregister.html.

[28] Meteonorm, Meteotest, Bern, Switzerland, 2014.

[29] Amt für Raumentwicklung, Bodenbedeckung, Zurich, 2015. www.are.zh.ch.

[30] Federal Office of The Environment, Hydrogeological Atlas of Switzerland, Zurich, n.d.

[31] Amt für Raumentwicklung, Wärmenutzung, Zurich, 2015. www.are.zh.ch.

[32] D. Wang, K. Orehounig, J. Carmeliet, Dynamic building energy demand modelling at urban scale for the case of Switzerland, in: CLIMA 2016 - Proc. 12th REHVA World Congr., 2016.

[33] D. Crawley, C. Pedersen, EnergyPlus: energy simulation program, ASHRAE J. 42 (2000) 49–56.

[34] K. Kavanaugh, Steve; Rafferty, Geothermal Heating and Cooling, Design of Ground-Source Heat Pump Systems, ASHRAE, 2014.

[35] M.A. Bernier, Closed-Loop Ground-Coupled Heat Pump Systems Ground Heat Exchanger Length, ASHRAE J. (2006).

[36] P. Eskilson, Thermal Analysis of Heat Extraction Boreholes, Response. (1987) 222.

[37] H.Y. Zeng, N.R. Diao, Z.H. Fang, A finite line-source model for boreholes in geothermal heat exchangers, Heat Transf. - Asian Res. 31 (2002) 558–567. doi:10.1002/htj.10057.

[38] L. Lamarche, B. Beauchamp, A new contribution to the finite line-source model for geothermal boreholes, Energy Build. 39 (2007) 188–198. doi:10.1016/j.enbuild.2006.06.003.

[39] L. Lamarche, A fast algorithm for the hourly simulations of ground-source heat pumps using arbitrary response factors, Renew. Energy. 34 (2009) 2252–2258. doi:10.1016/j.renene.2009.02.010.

[40] A.D. Chiasson, Geothermal Heat Pump and Heat Engine Systems: Theory And Practice Wiley-ASME Press Series, John Wiley & Sons, 2016, 2016.

[41] C. Yavuzturk, A Short Time Step Response Factor Model for Vertical Ground Loop Heat Exchangers, ASHRAE Trans. 105 (1999) 475–485.

[42] M. Bernier, P. Pinel, R. Labib, R. Paillot, A Multiple Load Aggregation Algorithm for Annual Hourly Simulations of GCHP Systems, HVAC&R Res. 10 (2004) 471–487. doi:10.1080/10789669.2004.10391115.

[43] M. Jakob, K. Flurry, N. Gross, G. Martius, B. Sunarjo, Kurzbericht Konzept Energieversorgung 2050: Szenarien für eine 2000-Watt-kompatible Wärme-versorgung für die Stadt Zürich, 2014.